EPJ Web of Conferences **314**, 00027 (2024) https://doi.org/10.1051/epjconf/202431400027
QCD@Work 2024

Renormalized Entanglement Entropy and general entropic c−function

Mitsutoshi Fujita[1,*], *Song* He[2,3,**], and *Yuan* Sun[4,***] *Jun* Zhang[5,****]

[1]School of Nuclear Science and Technology, University of South China, Hengyang 421001, China
[2]Center for Theoretical Physics and College of Physics, Jilin University, Changchun 130012, People's Republic of China
[3]Max Planck Institute for Gravitational Physics (Albert Einstein Institute), Am Mühlenberg 1, 14476 Golm, Germany
[4]School of Physics and Electronics, Central South University, Changsha 418003, China
[5]Department of Physics and Astronomy, University of Alabama, 514 University Boulevard, Tuscaloosa, AL, 35487, USA

Abstract. Holographic entanglement entropy (EE) and its renormalized form in AdS solitons with gauge potential are computed across a range of dimensions. The renormalized EE is identified as a cutoff-independent universal component of EE. By taking into account Kaluza-Klein reduction and the constraints of the low-energy limit, the $(d-1)$-dimensional renormalized EE is deduced from the odd-dimensional counterpart. The region associated with the shrinking circle, which is examined at large values of l is indicative of this relationship. Transitions of the minimal surface are from a disk-shaped to a cylindrical configuration as l increases. A quantum phase transition occurs at a critical subregion size, with the renormalized EE exhibiting non-monotonic behavior in the vicinity of this size. In all dimensions, massive modes become decoupled at the low energy limit, whereas degrees of freedom that include Wilson lines influence the behavior at smaller energy scales.

1 Introduction

Quantum entanglement entropy is a pivotal concept in quantum mechanics, offering valuable insights into the entanglement phenomenon between distant parts of a quantum system. By examining the entanglement among different elements, EE gives a metric for the extent of information. Its implications involve quantum information theory, black hole physics, and condensed matter physics. Specifically, the EE of a subsystem A reveals the level of entanglement within a given quantum field theory, as referenced in the literature [1, 2]. The geometric aspect of field theories is captured as an area law, which resembles black hole entropy.

A motivation of this research is to analyze quantum entanglement of quantum field theory (QFT) with negative energy. $d = 4$ $\mathcal{N} = 4$ SYM theory on S^1 has negative energy. Because scalar and fermions become massive in addition to S^1 component of the gauge field, the IR

*e-mail: fujitamitsutoshi@usc.edu.cn
**e-mail: hesong@jlu.edu.cn
***e-mail: sunyuan@csu.edu.cn
****e-mail: jzhang163@crimson.ua.edu

behavior of this theory is dominated by $d = 3$ pure Yang-Mills theory [3]. A feature of this theory is confinement and a mass gap. The AdS soliton is dual to confining theory via the AdS/CFT. The mass of the AdS soliton gives negative values, which corresponds to the negative Casimir energy of gauge theory on the boundary $S^1 \times R^{1,2}$. Thus, the AdS soliton is stabler than other background satisfying the same asymptotic boundary conditions.

Degrees of freedom can be also computed from EE. For example, the coefficient of the logarithmic term gives the A-type anomaly for a spherical entangling surface in conformal field theory (CFT) [4]. Renormalized EE with a spherical entangling surface generally becomes central charge in CFT [5]. In the context of $4d$ CFT, it becomes the A-type anomaly, which obeys the C-theorem: the renormalized EE decreases in the infrared limit. The entropic C function from the EE with the striped subsystem also becomes degrees of freedom and the central charge of CFT [6]. What is then the difference between two entropy? The trace anomaly part is different. Renormalized EE only contains either A-type or B-type anomaly, while entropic c function contains both A-type and B-type anomalies due to the coexistence of these two anomalies.

In this study, we delve into the B-type anomaly of QFT dual to the AdS soliton with the gauge potential by using renormalized EE. Our findings reveal that the renormalized EE exhibits non-monotonic behavior relative to the length of the interval. There is the signified occurance of a quantum phase transition between disk and cylinder topologies. Notably, this phase transition occurs not at free theory but at QFT in the large N limit. We show that renormalized EE is a probe of alternations in the operator mass and the gauge potential. Consequently, the renormalized EE diminishes as the operator mass increases, showing the decoupling of massive degrees of freedom.

In section 2, the UV structure of the entanglement entropy is analyzed. In section 3, the renoramlized EE is analyzed in 4-dimensions. In section 4, holographic stress tensors in the AdS soliton with gauge potential is reviewed. In section 5, renormalized EE of QFT dual to AdS solitons with gauge potential is analyzed. The quantum phase transition of renormalized EE is captured.

2 The UV structure of the entanglement entropy

The ultraviolet (UV) structure of EE encompasses the most signifinant divergent component, which is proportional to the area of the entangling surface. We define s_{UV} as the UV structure of EE with the entangling surface $S^1 \times S^{d-3}$, whereas $s^{(0)}_{UV}$ is the UV structure of EE with the entangling surface S^{d-2}. These two structures are interconnected by a specific relationship [7]:

$$s_{UV} = \frac{l_\phi}{r} s^{(0)}_{UV}, \tag{1}$$

where l_ϕ is the periodicity of S^1 and r is the radius of a sphere.

The renormalized entanglement entropy is obtained by a combination of differentiation. The renormalized entanglement entropy is finite and independent of the UV cut-off.

$$\begin{aligned} s_{ren} &= \frac{1}{r} f_d(r\partial_r) r s_{EE} = L_d(r\partial_r) s_{EE} \\ &= \begin{cases} \dfrac{1}{(d-2)!!} r\partial_r(r\partial_r - 2)\ldots(r\partial_r - (d-3)) s_{EE}, & d = \text{odd}, \\ \dfrac{1}{(d-2)!!} (r\partial_r + 1)(r\partial_r - 1)\ldots(r\partial_r - (d-3)) s_{EE}, & d = \text{even}, \end{cases} \end{aligned} \tag{2}$$

Note that the first line is equal to $d-1$ dimensional renormalized entanglement entropy with the entangling surface S^{d-2} as follows [5]:

$$f_d(r\partial_r)s^{(0)}_{EE} = \begin{cases} \frac{1}{(d-2)!!}(r\partial_r - 1)(r\partial_r - 3)\dots(r\partial_r - (d-2))s^{(0)}_{EE}, & d = \text{odd}, \\ \frac{1}{(d-2)!!}r\partial_r(r\partial_r - 2)\dots(r\partial_r - (d-2))s^{(0)}_{EE}, & d = \text{even}. \end{cases} \tag{3}$$

We focus on odd dimensional results. According to (2), the renormalized entanglement entropy for $d = 3$ and $d = 5$, becomes

$$s_{ren} = r\partial_r s_{EE} \quad \text{for } d = 3, \tag{4}$$

$$s_{ren} = \frac{1}{3}r\partial_r(r\partial_r - 2)s_{EE} \quad \text{for } d = 5. \tag{5}$$

OUr analysis reveals that through a Kaluza-Klein reduction along the S^1 direction, the renormalized entanglement entropy effectively embodies $d-1$ dimensional one in the infrared limit. The first formula resembles the form of the 2-dimensional entropic c function, which is known to be non-negative and exhibits monotonic decrease in systems respecting Lorentz symmetry. In our study, we demonstrate that (4) in $d = 3$ adheres to these properties for QFT dual to the deformed AdS soliton. Conversely, the behavior of the $4d$ renormalized entanglement entropy exhibits non-monotonic characteristics.

3 Renormalized entanglement entropy of 4d QFT

In this section, we examine the entanglement entropy and renormalized entanglement entropy across various scenarios, including a free scalar, Dirac fermion, and a 4-dimensional CFT. The trace anomaly in general CFT is linked to the logarithmic term inherent to EE.

The length scale r_1 of the subregion is related to rescaling of the metric:

$$\begin{aligned} r_1\partial_{r_1}s_{EE} &= \lim_{n\to 1}(-2\partial_n \int d^{d+1}x g_{\mu\nu}(x)\frac{\delta}{\delta g_{\mu\nu}(x)}[w - nw|_{n=1}]) \\ &\frac{1}{2\pi}\lim_{n\to 1}\partial_n\Big(\langle\int d^{d+1}x\sqrt{g}T_\mu{}^\mu(x)\rangle_{M_n} - n\langle\int d^{d+1}x\sqrt{g}T_\mu{}^\mu(x)\rangle_{M_1}\Big), \end{aligned} \tag{6}$$

where w is the effective action in the manifold with conical singularities M_n. EE has been replaced with a function of the partition function in M_n. The formula (6) relates EE to the trace anomaly.

To compute EE, we focus on a subsystem σ which is a cylindrical configuration where one direction is S^1. This subsystem aligns with the one in QFT corresponding to $d+1$-dimensional AdS solitons. By integrating the formula (6) and applying the trace anomaly formula, the log term of the entanglement entropy [8, 9] becomes $S_{EE} = s_A \log\big(\epsilon/R_1\big)$, where s has expression with respect to extrinsic curvatures [4]

$$s_A = \frac{a}{180}\int_{\partial\sigma} d^2x\sqrt{h}E_2 + \frac{c}{120}\int_{\partial\sigma} d^2x\sqrt{h}I_2, \tag{7}$$

where E_2 is the Euler density and I_2 is a Weyl invariant. Compared with the normalization of , $a = 360a_4$ and $c = 120c_4$. For a real scalar, $c = 1$ and for Dirac fermion, $c = 6$. Coefficients agree with trace anomalies.

The renormalized entanglement entropy for cylinder type topology in (2) becomes

$$S_{ren} = \frac{1}{2}(r\partial_r + 1)(r\partial_r - 1)s_{EE} = s_A = \frac{cl_\phi}{240r}. \tag{8}$$

Thus, the renormalized EE is consistent with the coefficient s_A. The renormalized entanglement entropy for a spherical entangling surface (3) becomes

$$S_{ren} = \frac{1}{2} r\partial_r (r\partial_r - 2) s_{EE} = s_A = \frac{a}{90}. \tag{9}$$

According to [5], the renormalized EE is consistent with s once again.

4 The AdS soliton with the gauge potential

The AdS soliton arises from performing a double Wick rotation of the AdS black hole. It corresponds to QFT with anti-periodic boundary conditions on fermions. The mass of the AdS soliton equates to the negative energy of the corresponding dual QFT [11]. This methodology has been applied for the Reissner Nordstrom AdS black hole as reported in reference [12]. An analytic continuation of the metric across both temporal and spatial dimensions is performed. The metric of the AdS soliton with a background gauge field becomes [13]

$$\begin{aligned} ds^2_{d+1} =& \frac{L^2}{z^2}\Big(\frac{dz^2}{h(z)} + h(z)d\phi^2 - dt^2 + dR^2 + R^2 d\Omega_{d-3}\Big), \\ A_\phi =& a_\phi^{(0)}\Big(1 - \Big(\frac{z}{z_+}\Big)^{d-2}\Big), \end{aligned} \tag{10}$$

where

$$h(z) = 1 - \Big(1 + \tilde{\epsilon} z_+^2 a_\phi^2\Big)\Big(\frac{z}{z_+}\Big)^d + \tilde{\epsilon} z_+^2 a_\phi^2 \Big(\frac{z}{z_+}\Big)^{2(d-1)}. \tag{11}$$

Here, we set $\tilde{\epsilon} = -1$ [1], The gauge field becomes as the source field of the conserved current and gives a non-zero VEV for the current $\langle J_\phi \rangle$. This gauge field becomes a Wilson line, changing the boundary condition (twisted boundary condition), by considering a gauge transformation. The Wilson line approaches to zero at the tip $z = z_+$ and the gauge connection is regular there. The radial coordinate is restricted to $z \le z_+$.

Due to the regularity at the tip of the cigar, ϕ must have the periodicity $\phi \to \phi + 1/m_0$, where the Kaluza-Klein mass is defined as

$$m_0 = \frac{1}{4\pi z_+}\Big(d + (d-2)\frac{a_\phi^2}{z_+^2}\Big). \tag{12}$$

When one rewrites (12) with respect to m_0 and a_ϕ, there is a bound between two. The solution exists only if

$$a_\phi \le \frac{2\pi m_0}{\sqrt{d(d-2)}} = a_c. \tag{13}$$

According to [10], the boundary energy becomes

$$M = -\frac{V_{d-2}}{m_0}\frac{L^{d-1}\bar{a}_\phi}{2\kappa^2 z_+^d}. \tag{14}$$

The boundary energy can become negative or positive depending on Wilson lines (gauge potential),.

$$\begin{cases} M < 0 & z_+ a_\phi < 1 \\ M > 0 & z_+ a_\phi > 1. \end{cases} \tag{15}$$

For $a_\phi = 0$, it becomes Casimier energy of dual $4d$ Super Yang-Mills theory [11]. Casimir energy is different among periodic, anti-periodic boundary conditions, and twisted boundary conditions.

[1] $\tilde{\epsilon} = 1$ for the Reissner Nordstrom AdS black hole.

5 The holographic entanglement entropy

Figure 1. The minimal surface for the small (left) and large (right) subregion in the gravitational background. Since the subregion is a spherical region, the minimal surface becomes a disk (cylinder) type of the small (large) subregion.

In this section, we compute the holographic entanglement entropy. We choose the entangling surface $S^1 \times S^{d-3}$: $R = r$ and $0 \leq \phi \leq l_\phi$ at a fixed time instance in the background (10). $R = R(z)$ is utilized as an embedding scalar. Note that this choice of entangling surface differs from those scenarios without the compactification of the ϕ direction. The surface action becomes

$$A = \int d^{d-1}x\mathcal{L} = \Omega_{d-3} l_\phi L^{d-1} \int dz \frac{R^{d-3}}{z^{d-1}} \sqrt{1 + h\dot{R}^2}, \tag{16}$$

where $\mathcal{L} = \sqrt{\det g_{ind}}$ and g_{ind} is the induced metric. The holographic entanglement entropy is given by

$$s^g_{EE} = \frac{2\pi}{\kappa^2} A \tag{17}$$

where A is minimized. Recall that the ratio L^{d-1}/κ^2 is dimensionless. We solve the EOM derived from (16). For this purpose, boundary conditions are imposed on $R(z)$. We consider two kinds of boundary conditions. The first one is a Disk type boundary conditions: $R(z_t) = 0$ and $R'(z_t) = \infty$. The second one is a cylinder type boundary condition: $z_t = z_+$. The minimal surface of each a type is written in Fig. 1 taken from [14].

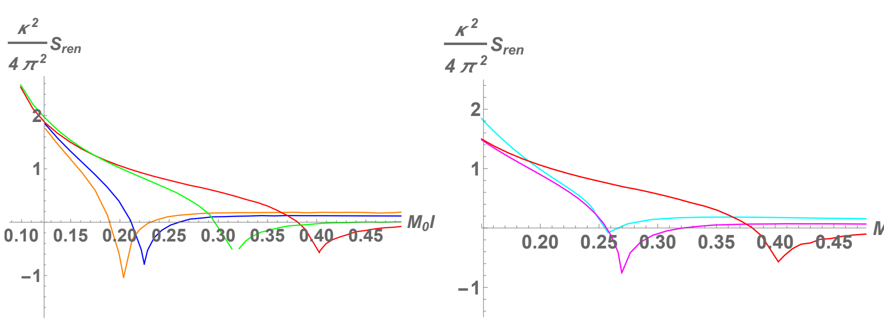

Figure 2. S_{ren} in 4 dimensions. (Left) S_{ren} for $d = 4$ is plotted for $a_\phi = \frac{i}{2},\ 0,\ \frac{2}{3},\ \frac{1}{\sqrt{2}}$ from the left to the right. The quantum phase transition occurs for $m_0 r_c = 0.21,\ 0.23,\ 0.32,\ 0.4$. Renormalized EE non-monotonically behaves around critical lengths. (Right) Renormalized EE for $m_0 = 3/5,\ 2/5,\ 1/\pi$ from the left to the right. The quantum phase transition occurs when $m_0 r_c = 0.24,\ 0.27,\ 0.4$. It implies that massive modes decouple others as soon as possible. The final state becomes a product state.

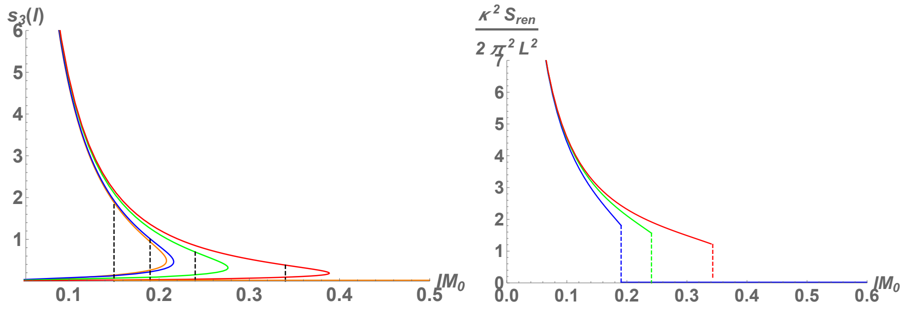

Figure 3. Left: $s_3(r) = dA_s/(3l_\phi dr)$ is plotted as a function of rm_0 for $a_\phi = i/2,\ 0,\ 1,\ 2/\sqrt{3}$ from the left to the right. The phase transition occurs at critical lengths $r_c = 0.15,\ 0.19,\ 0.24,\ 0.34$. $s_3(r)$ has multi-values. The upper curve agrees with the strong subadditivity. Right: S_{ren} for $d = 3$ for $a_\phi = 0,\ 1,\ 2/\sqrt{3}$ from the left to the right. S_{ren} monotonically decreases as a function of rm_0 and jumps to zero at a large distance. It implies that theory is a product state there.

For $4d$, renormalized EE is given by the formula (2), in which the differentiation is applied to s^g_{EE}. Renormalized EE is indicative of effective degrees of freedom from EE at energy scale $E \sim 1/r$. Renormalized EE is dipicted as a function of rm_0 ($r \equiv l$) in Fig. 2 sourced from [14]. Renormalized EE non-monotonically behaves near the critical length, which is analogous to a behavior of GPPZ flow. Because degrees of freedom with Wilson lines remain at large a_ϕ and high energy, the renormalized EE slowly decreases until the critical length. For low energies, the renoramlized EE fails to discern the effective degrees of freedom and almost stabilizes to a constant value. It implies that Wilson lines make particles of dual QFT light. The right figure shows that massive modes decouple others soon.

For $3d$, renormalized EE is plotted as a function of rm_0 in Fig. 3 taken from [14]. Renormalized EE is positive and monotonically decreasing because massive degrees of freedom decouple others in the low energy limit. This monotonic behavior arises because of Lorentz symmetry and strong subadditivity. The quantum phase transition occurs at critical lengths. Figures are consistent with the entropic c function in $R^{1,1}$. In the left Figure, $s_3(r)$ is ds_{EE}/dr. Figures also reflect that the minimal surface is concave.

6 Discussion

Renormalized EE exhibits a non-monotonic trend around a critical length, while it partially satisfies C-theorem because $S_{ren}(r \to 0) \geq S_{ren}(r \to \infty)$. S^{ren} in the small length limit is larger than S^{ren} in the large length limit. Only for $d = 3$, REE decreases and becomes positive because of its form $S_{ren} = r\partial r s^{EE}$ constrained by Lorentz invariance and strong subadditivity. [2] Renormalized EE also counts effective DOF of Wilson lines along the S^1 direction, capturing quantum phase transition.

Except for $d = 3$, qualitative behavior of renormalized EE is analogous to the generalized entropic C-function. Both quantities count effective DOF of Wilson lines and detect quantum phase transition. For $d = 3$, renormalized EE is different from the generalized entropic C-function by a product of r: $C^g = rS^{d=3}_{ren}$. Actually, the non-monotonic behavior of the generalized entropic C-function can be attributed to the interplay between r and $\partial s_{EE}/\partial r$.

[2] We would like to thank T. Takayanagi for pointing out this.

References

[1] C. Holzhey, F. Larsen and F. Wilczek, "Geometric and renormalized entropy in conformal field theory," Nucl. Phys. B **424**, 443 (1994) [arXiv:hep-th/9403108]; P. Calabrese and J. L. Cardy, "Entanglement entropy and quantum field theory," J. Stat. Mech. **0406**, P002 (2004) [arXiv:hep-th/0405152]

[2] P. Calabrese and J. Cardy, "Entanglement entropy and conformal field theory," J. Phys. A **42** (2009) 504005 [arXiv:0905.4013 [cond-mat.stat-mech]]; H. Casini and M. Huerta, "Entanglement entropy in free quantum field theory," J. Phys. A **42** (2009) 504007 [arXiv:0905.2562 [hep-th]]

[3] E. Witten, "Anti-de Sitter space, thermal phase transition, and confinement in gauge theories," Adv. Theor. Math. Phys. **2**, 505-532 (1998) [arXiv:hep-th/9803131 [hep-th]]

[4] S. N. Solodukhin, "Entanglement entropy, conformal invariance and extrinsic geometry," Phys. Lett. B **665**, 305-309 (2008) [arXiv:0802.3117 [hep-th]]

[5] H. Liu and M. Mezei, "A Refinement of entanglement entropy and the number of degrees of freedom," JHEP **04** (2013), 162 [arXiv:1202.2070 [hep-th]]

[6] T. Nishioka and T. Takayanagi, "AdS Bubbles, Entropy and Closed String Tachyons," JHEP **0701**, 090 (2007) [hep-th/0611035]

[7] M. Ishihara, F. L. Lin and B. Ning, "Refined Holographic Entanglement Entropy for the AdS Solitons and AdS black Holes," Nucl. Phys. B **872**, 392-426 (2013) [arXiv:1203.6153 [hep-th]]

[8] H. Casini and M. Huerta, "Entanglement entropy in free quantum field theory," J. Phys. A **42**, 504007 (2009) doi:10.1088/1751-8113/42/50/504007 [arXiv:0905.2562 [hep-th]]

[9] M. Huerta, "Numerical Determination of the Entanglement Entropy for Free Fields in the Cylinder," Phys. Lett. B **710**, 691-696 (2012) [arXiv:1112.1277 [hep-th]]

[10] V. Balasubramanian and P. Kraus, "A Stress tensor for Anti-de Sitter gravity," Commun. Math. Phys. **208**, 413 (1999) [hep-th/9902121]

[11] G. T. Horowitz and R. C. Myers, "The AdS / CFT correspondence and a new positive energy conjecture for general relativity," Phys. Rev. D **59**, 026005 (1998) [hep-th/9808079]

[12] S. A. Hartnoll, "Lectures on holographic methods for condensed matter physics," Class. Quant. Grav. **26**, 224002 (2009) [arXiv:0903.3246 [hep-th]]

[13] M. Fujita, S. He and Y. Sun, "Thermodynamical property of entanglement entropy and deconfinement phase transition," Phys. Rev. D **102** (2020) no.12, 126019 [arXiv:2005.01048 [hep-th]]

[14] M. Fujita, S. He, Y. Sun and J. Zhang, "Holographic renormalized entanglement and entropic c-function," JHEP **01**, 079 (2024) [arXiv:2309.03491 [hep-th]]